Upstream and Downstream Co-inhibition of Mitogen-Activated Protein Kinase and PI3K/Akt/mTOR Pathways in Pancreatic Ductal Adenocarcinoma

CrossMark

Matthew H. Wong*[,†], Aiqun Xue*, Robert C. Baxter[‡], Nick Pavlakis[§] and Ross C. Smith*[,#]

*Cancer Surgery Research Laboratory, Kolling Institute of Medical Research, University of Sydney, Sydney, NSW, Australia; [†]Department of Medical Oncology, Gosford Hospital, Sydney, NSW, Australia; [‡]Hormones and Cancer, Kolling Institute of Medical Research, University of Sydney, Sydney, NSW, Australia; [§]Department of Medical Oncology, Royal North Shore Hospital, University of Sydney, Sydney, NSW, Australia; [#]Department of Upper Gastrointestinal Surgery, Royal North Shore Hospital, University of Sydney, Sydney, NSW, Australia

Abstract

BACKGROUND: Extensive cross talk exists between PI3K/Akt/mTOR and mitogen-activated protein kinase (MAPK) pathways, and both are upregulated in pancreatic ductal adenocarcinoma (PDAC). Our previous study suggested that epidermal growth factor receptor inhibitor erlotinib which acts upstream of these pathways acts synergistically with PI3K inhibitors in PDAC. Horizontal combined blockade upstream and downstream of these two pathways is therefore explored. *METHODS:* Erlotinib paired with PI3K inhibitor (BYL719) was tested against erlotinib plus dual PI3K/mTOR inhibitor BEZ-235, and MEK inhibitor (PD98059) plus BEZ235, on five primary PDAC cell lines and on two pairs of parent and erlotinib-resistant (ER) cell lines. A range of *in vitro* assays including cell proliferation, Western blotting, migration, clonogenic, cell cycle, and apoptotic assays was used to test for the efficacy of combined blockade. *RESULTS:* Dual downstream blockade of the MAPK and PAM pathways was more effective in attenuating downstream molecular signals. Synergy was demonstrated for erlotinib and BEZ235 and for PD-98059 and BEZ-235. This resulted in a trend of increased growth cell cycle arrest, apoptosis, cell proliferation, and colony and migration suppression. This combination showed more efficacy in cell lines with acquired resistance to erlotinib. *CONCLUSIONS:* The additional mTOR blockade provided by BEZ235 in combined blockade resulted in increased anticancer effect. The hypersensitivity of ER cell lines to additional mTOR blockade suggested PAM pathway oncogenic dependence via mTOR. Dual downstream combined blockade of MAPK and PAM pathways with MEK and PI3K/mTOR inhibitor appeared most effective and represents an attractive therapeutic strategy against pancreatic cancer and its associated drug resistance.

Neoplasia (2016) 18, 425–435

Introduction

Pancreatic ductal adenocarcinoma (PDAC) is a deadly disease that is often diagnosed late, has limited chemotherapeutic options, and has relatively poor survival. Even though K-Ras; CDKN2A/P16, P53; and SMAD4 have already been identified as the four core molecular pathways disrupted in PDAC since the early 2000s, there has been little advance in targeted therapy in this cancer [1–3]. The only targeted therapy with proven efficacy to date is the epidermal growth

factor receptor (EGFR) tyrosine kinase inhibitor (TKI) erlotinib in the PA.3 trial. In this trial, gemcitabine plus erlotinib delayed progression by 23% ($P = .004$) and improved overall survival by 18% ($P = .038$). However, the absolute benefit was exceedingly small, with 0.2-month and 10-day gain in median progression-free survival and overall survival [4]. There are a number of reasons that may potentially explain the failure of targeted therapy in pancreatic cancer.

One reason has been attributed to intratumoral heterogeneity, where subclonal population driven by genomic instability acquires frequent mutations through evolutionary process, resulting in extensive genetic diversity [5]. This is certainly supported by the findings of the Australian Pancreatic Genome Initiative, which found over 2000 nonsilent mutations and 1600 copy number variations in 142 pancreatic cancer tumors and an average of 26 mutations per patient [6]. That said, the vast majority of homozygous mutations (89%) already existed in the parental clone of PDAC, and deleterious mutations were more commonly found in parent than subclones (12.6% vs 8.1%) in a concurrent primary-metastases study [7]. Another explanation given for the failure of targeted therapy when used empirically is the failure to identify a sensitive subgroup due to the lack of predictive biomarkers. The lack of success is not restricted to targeted therapy such as K-Ras mutation and EGFR copy number in the use of erlotinib [8], but also with hENT1 in the use of gemcitabine and SPARC-1 in the use of abraxane chemotherapy [9–11]. The initial excitement in these biomarker developments was met with disappointment in validation studies of prospective phase III trials. This failure emphasizes likely heterogeneity in drug resistance mechanisms in PDAC and that these mechanisms are not of key importance in driving growth or drug sensitivity. An alternative explanation is that the extensive cross talk between redundant oncogenic pathways in this cancer allows pathway blockade to be easily circumvented [12]. Of these, cross talk between the mitogen-activated protein kinase pathway (MAPK) and the PI3K/Akt/mTOR (PAM) pathway appears particularly important clinically. These appear to be particularly important for promoting cancer cell growth, proliferation, survival, and migration (Supp Figure 1). The extensive cross talk between MAPK and PAM pathways may explain the relative low efficacy of PI3K inhibitors and the apparent cytostaticity of MEK inhibitors, which in turn suggests potential benefits in a horizontal combined blockade (CB) strategy [13,14].

Preclinical studies have demonstrated the effectiveness of MAPK-PAM co-inhibition in suppressing feedback loops associated with reactivation of the reciprocal pathway [15] and also established synergy between the dual inhibitors in B-Raf mutated melanoma, K-Ras mutated colorectal cancer, PTEN deleted ovarian cancer, lung cancer, and triple-negative breast cancer [13]. In our previous study, erlotinib was shown to act synergistically with the PI3Kα inhibitor BYL-719. *In vitro*, the combined EGFR-PI3K blockade resulted in growth cell cycle arrest and apoptosis, and was effective in suppressing colony formation and cell migration. *In vivo*, this significantly inhibited tumor growth compared with control treatment in subrenal and subcutaneous patient-derived xenograft tumor models [16]. However, the previous study only concentrated on EGFR-insulin-like growth factor-1 receptor (IGF1R) versus EGFR-PI3K CB. Furthermore, it was uncertain whether PI3K/Akt signaling was the key molecular pathway conferring onocogenic dependence in pancreatic cancer or whether a downstream molecular signal such as mTOR was responsible for it. Given the premise of the cross-interaction between the MAPK and PAM pathways downstream, the current study was undertaken to investigate the efficacy of three CBs (EGFR-PI3K, EGFR-PI3K/mTOR, MEK-PI3K/mTOR) on a range of cellular functions of pancreatic cancer primary and acquired resistant cell lines. The aim was firstly to investigate the role of additional mTOR inhibition in CB, secondly to understand the pathophysiology of resistance and oncogenic dependence in relations to the upstream and downstream signals of the PAM and MAPK pathways, and thirdly to find the optimal combined therapy to take into clinical trials.

Materials and Methods

PDAC Cell Lines and Inhibitors

BxPC-3, CFPAC-1, CAPAN-2, MiaPACA-2, and PANC-1 cells were purchased from ATCC (Manassas, VA). Cell lines were typed by short tandem repeat profiling, and they conformed to the ATCC reference standards (CellBank, Westmead, NSW, Australia). Two erlotinib-resistant (ER) cell lines were subcultured from BxPC-3 and PANC-1, respectively, after treatment daily with graduating concentrations of erlotinib (ERL) from 10 to 30 μM over a 10-month period. The final ER cell lines (BxPC-ER and PANC-ER) showed a 349% and 273% increase in erlotinib IC_{50} compared with parent cell lines and were retyped to ensure the same ATCC standards, screened for contamination, and had IC_{50} retested after 4 weeks of culturing under normal conditions to ensure the stability of these cell lines to drug resistance. Erlotinib (Selleckchem, Scoresby, VIC, Australia), NVP-BYL719 (BYL; Novartis, Basel, Switzerland), NVP-BEZ235 (BEZ; Novartis, Basel, Switzerland), and PD-98059 (PD; Selleckchem) were dissolved in 100% DMSO as 20-mM, 10-mM, 100-μM, and 4-mM stock solutions, respectively, and frozen at −20°C. The cell lines and inhibitors used in each respective experiment are shown in Supplementary Table 1.

Cell Proliferation and Confluence Assays

Cells were seeded at 2×10^3 density in 100 μl final volume in 96-well plates and treated with inhibitors for 72 hours. Cytotoxic IC_{50} was first determined for each inhibitor on the five primary PDAC cell lines, and average IC_{50av} was calculated. The dose intensity of combined treatment was set at 50% of IC_{50av} of each respective drug (final concentration). Cells were then treated with single and combined blockade in a 6×6 dosing matrix. The MTT assay was used to measure viability after 72-hour treatment (BioTek Synergy HT, Winooski, VT) [17]. For illustration and comparison, three doubling dosing levels of CB (low, medium, and high concentration) are presented in column graphs: ERL + BYL or EY (E 5 μM + Y 2.5 μM, E 10 μM + Y 5 μM, E 20 μM + Y 10 μM), ERL + BEZ or EB (E 5 μM + B 0.05 μM, E 10 μM + B 0.1 μM, E 20 μM + B 0.2 μM), and PD + BEZ or PB (PD 5 μM + B 0.05 μM, PD 10 μM + B 0.1 μM, PD 20 μM + B 0.2 μM). For the study of synergy, three-dimensional surface plots were fitted with 36 data points of each of the quadruplicate experiments using spline interpolation (SAS 9.2), and synergy indices (SIs) with confidence intervals (CIs) were calculated using nonlinear regression algorithm on a four-parameter Bliss model as described previously (SAS 9.2) [18]. The data were also analyzed as percentage of confluence compared with untreated control for comparison of treatment doses on the confluence of cells.

Western Blotting

Western blotting was conducted as previously described [19]. BCA Protein Assay (Thermo Fisher, Scoresby, VIC, Australia) was used to adjust protein concentrations. Dual inhibitors at the highest set concentration were added for 60 minutes followed by 10 minutes of

growth factor stimulation [EGF, 10 ng/ml (Sigma, Castle Hill, NSW, Australia) and IGF-I, 50 ng/ml (Sigma)]. The primary antibodies for pERK, ERK, pAkt, Akt, pS6, S6, and β-actin were from Cell Signaling. Secondary antibodies (goat anti-rabbit and goat anti-mouse) were from Santa Cruz (Mulgrave, VIC, Australia).

Cell Cycle Assay (Flow Cytometry)

Cells were treated with the 3 CB combinations at lowest set concentration for 48 hours. A total of 300 μl each of flow cytometry cell cycle mixture was added to the samples after discarding supernatants from centrifuged samples. The flow cytometry mixture consisted of 50 μg/ml of propidium iodide (PI), 25 μg/ml of fresh boiled RNase, and 0.2% Triton X-100 in PBS. Cell cycle distribution was analyzed by the two-laser four-color FACS Calibus (BD Bioscience, San Jose, CA) on the FL2-A channel (designated to DNA mass by PI). DNA histograms were constructed by Modfit (Verity, Topsham, ME). The percentage of cells in S-phase [S-phase fraction (SPF)] was used as the end point of this study.

Apoptosis Assay (Flow Cytomtery)

Cells were treated with the same low-concentration CB combination and suspended in 300 μl of PBS. To each sample, 2 μl of 2 μM DiLC1(5) (Sapphire Bioscience, Sydney, Australia) and 10 μg/ml PI were added for 30 minutes. DiLC1(5) fluorescence was excited at 633 nm, and PI was excited at 488 nm. Apoptotic cells had a clear loss of mitochondrial signal but retained intact cell membranes and were located on the lower left quadrant of the apoptosis scatterplots. Necrotic cells had lost the mitochondrial signal but were stained with PI because of disrupted cell membranes and were located in the lower right quadrant. Apoptotic and necrotic cells were analyzed together as they were usually found on a continuum of cell stress and cell death.

Clonogenic Assay (Anchorage Dependent Growth)

Cells (2000/well) were reseeded after 72-hour exposure to dual inhibitors and were allowed to grow for 7 to 10 days (10% confluence). Crystal violet (0.05%) was used to stain the cells, and images were taken on the LAS-3000 imaging system (Fujifilm, Brookvale, NSW, Australia). Colonies were counted using Colony v1.1 software (Fujifilm) and were represented as a percentage of colonies in untreated controls.

Migration Assay

A total of 8×10^5 cells were seeded in 96-well ImageLock plates (Essen Bioscience) to achieve 100% confluence and pretreated with mitomycin (10 μg/ml) as an antiproliferation agent. The Essen Bioscience 96-pin wound maker was used on the plate to make a uniform scratch in each well. After three washings, cells were incubated in a fresh medium mixture consisting of 10% FBS, 10 μg/ml mitomycin, and varying CB mixtures. The plate was inserted into the IncuCyte imager (Essen Bioscience), where images were taken every 2 hours for 40 hours using high-definition phase contrast. Cell migration kinetics were measured using relative migration density as calculated by the software provided.

Results

Maximal Suppression MAPK and PAM Pathways Signaling by MEK and PI3K/mTOR Co-inhibition

Among five PDAC cell lines, BxPC-3 and PANC-1 were selected to perform single versus combined blockade Western blotting experiments given that the former was RAS wild type and highly

sensitive to multiple TKI, whereas the latter was KRAS mutated at codon 12 and with intrinsic low sensitivity to TKI (Supplementary Figure 2). In BxPC-3, ERL appropriately reduced EGF-stimulated pEGFR and pERK at 10 ng/ml, whereas BYL reduced IGF-stimulated pAkt signals at 50 ng/ml. CB using either drug in combination with ERL on this cell line was capable of near-complete inhibition of pERK and pAkt in the presence of both EGF and IGF. In PANC-1, however, pAkt was either unaffected by ERL, whereas BYL appropriately decreased downstream signals. EY CB was able to attenuate most downstream signals including pERK, pAkt, and pS6, and the inhibition was nearly complete at high dose (ERL 20 μM and BYL 10 μM). In the EB experiments, BEZ alone hits the targets PI3K and mTOR, resulting in diminishing of AKT and disappearing of S6 (downstream of mTORC1) at a dose as low as 10 nM in both cell lines. On the other hand, in the PB experiments, PD was not a very good MEK inhibitor. It only began to decrease ERK (downstream of MEK) at 10 μM for BxPC-3, whereas PANC-1 was completely resistant to its effect on ERK. Despite the fact that PD was inferior to erlotinib in inhibiting the downstream MAPK pathway, either drug combined with BEZ resulted in some reduction in pERK signals in addition to disappearing of pAKT and pS6 in both cell lines. This confirmed the potency of BEZ by itself or in combination with EGFR or MEK inhibitor.

ER cell lines characterized by upregulated PAM pathways were developed previously [16]. The three CBs were further tested against each other in the two pairs of parent (BxPC-3, PANC-1) and ER cell lines (BxPC-ER and PANC-ER) (Figure 1A). The parent cell lines BxPC-3 and PANC-1 demonstrated increased pAkt and pS6 in response to high concentration EGF (20 ng/ml), which was further increased after these cell lines had acquired erlotinib resistance. This enhanced phosphorylation was abrogated by treatment with the three CBs upstream and downstream of MAPK and PAM pathways: EY, EB, and PB. These blockades corresponded to inhibition of EGFR-PI3K (EY), EGFR-PI3K/mTOR (EB), and MEK-PI3K/mTOR (PB). The most striking differences between the three CBs was that pAkt and pS6 were attenuated but still present with EGFR-PI3K co-inhibition, but both phosphorylated signals completely disappeared with EGFR-PI3K/mTOR and MEK-PI3K/mTOR co-inhibition (Figure 1A, straight arrows). This appeared more so in the ER cells compared with parent cell lines, implying that PI3Kα blockade alone was insufficient to switch off PAM pathway in cell lines with oncogenic shift to PI3K/Akt. pERK remained present in all three CBs during 20-ng/ml EGF stimulation, but again, the CBs that additionally inhibited mTOR (EB and PB) appeared to inhibit it more than EY, particularly in PANC-ER compared with PANC-1 (Figure 1A, dotted arrows). Figure 1B shows mean data from three of experiments of pERK, pAkt, and pS6 signal response to CB compared with EGF stimulation. As previously shown in Figure 1A, pAkt and pS6 signals were only weakly activated by EGF in BxPC-3, implying weak EGFR-PI3K cross talk in this cell line. Thus, the effects of all three CBs compared with EGF stimulation were all close to one. For the other cell lines, CB appeared to suppress downstream molecular signals and in general attenuate pAkt signals more than pERK and pS6, in keeping with the direct downstream targeting of PI3K/Akt. Comparing the three CBs, there was certainly some disparity in the effect of upstream/downstream CB on pERK and pAkt among the four cell lines. However, there was a consistent trend toward increasing suppression of pS6 for CB containing PI3K/mTOR inhibition (EB, PB) compared with that of PI3K inhibition only (EY) even though this did not result in statistical significance (Figure 1B, straight arrows). This is in keeping with the knowledge that pS6 is a downstream effector of
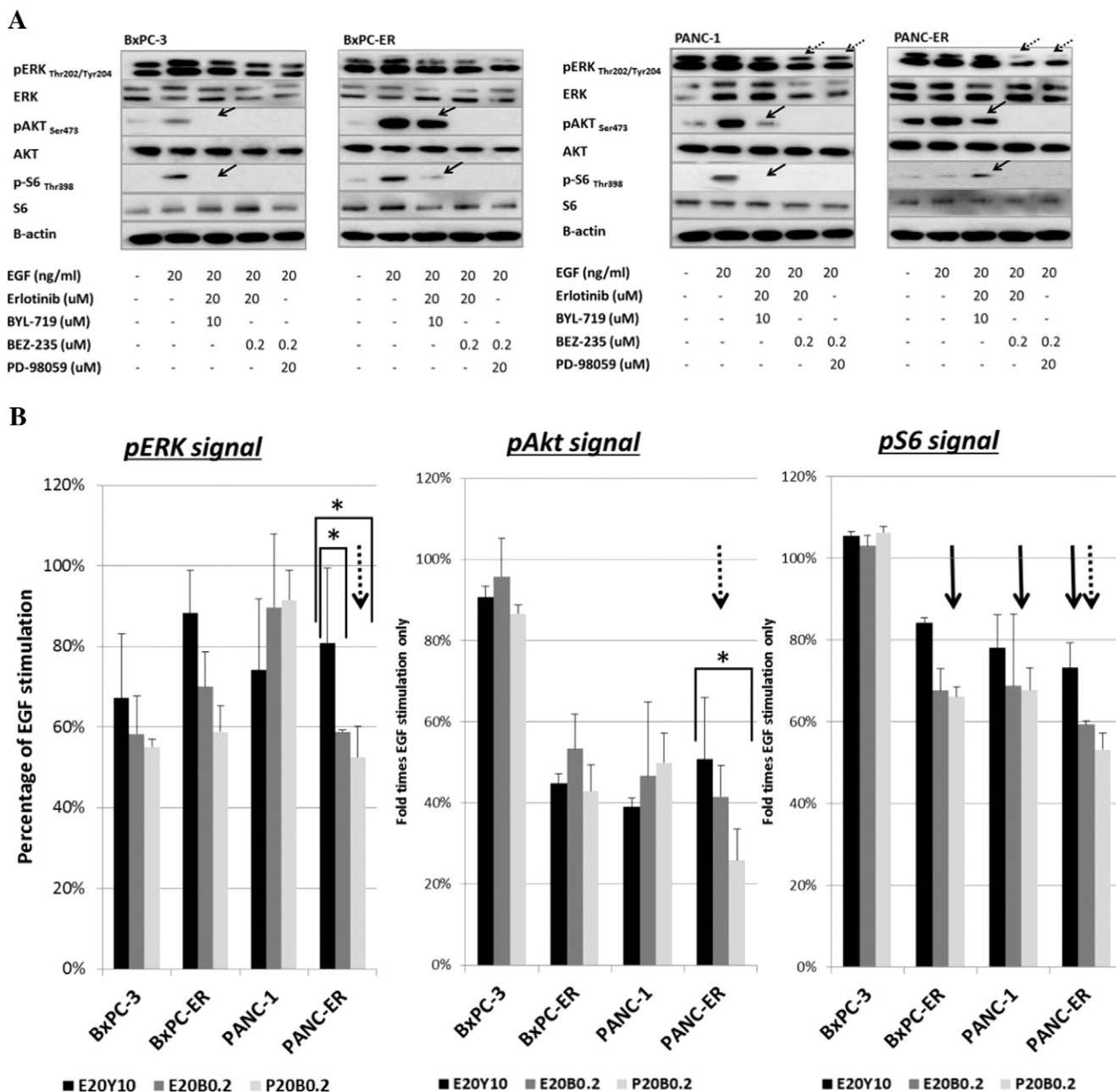
Figure 1. Effect of CB on Akt and S6 activation in pancreatic cancer cell lines. (A) Representative Western blots showing the effect of CB (high concentration) on pAkt and pS6 in BXPC-3 and PANC-1 and their respective ER cells. The straight arrows highlight the incomplete attenuation of pAKT and pS6 in the ER cells in response to CB with ERL and BYL. The dotted arrows indicate the reduced level of pERK in the ER cells with ERL added to BEZ or PD protocols. (B) Mean and SEM of three Western blot experiments comparing phosphorylation responses to CB (E20Y10 denotes ERL 20 μM + BYL 10 μM, E20B0.2 denotes ERL 20 μM + BEZ 0.2 μM, P20B0.2 denotes PD 20 μM + BEZ 0.2 μM in combination). Results were expressed as a percentage of EGF-stimulated values.

mTORC1, the direct signaling that is inhibited by the dual PI3K/mTOR inhibitor BEZ235. In addition, in PANC-ER which had been shown to be the most strongly Akt-upregulated cell line [16], both pERK and pAkt also followed the same pattern above (Figure 1B, *dotted arrows*) with statistically significant reduction in pERK signal in EB and PB compared with EY ($P = .036$ and $.048$) and in pAkt signal in PB compared with EY ($P = .035$). This suggests oncogenic dependency of this cell line on the downstream MAPK-PAM pathways, making it susceptible to MEK and mTOR blockade.

Growth Cycle Arrest and Apoptosis/Necrosis with Downstream CB

Because mTOR is intricately involved in cell cycle progression and cell survival [20,21], cell cycle and apoptosis assays using flow cytometry were performed to examine the effect of upstream versus downstream CB. Our previous study had already shown substantial impact of EY at medium concentration (ERL 10 + 5 μM) on G1 cycle arrest (down to 18%-22% SPF) and apoptosis (up to 75%-82% apoptosis plus necrosis), more so compared with single agent
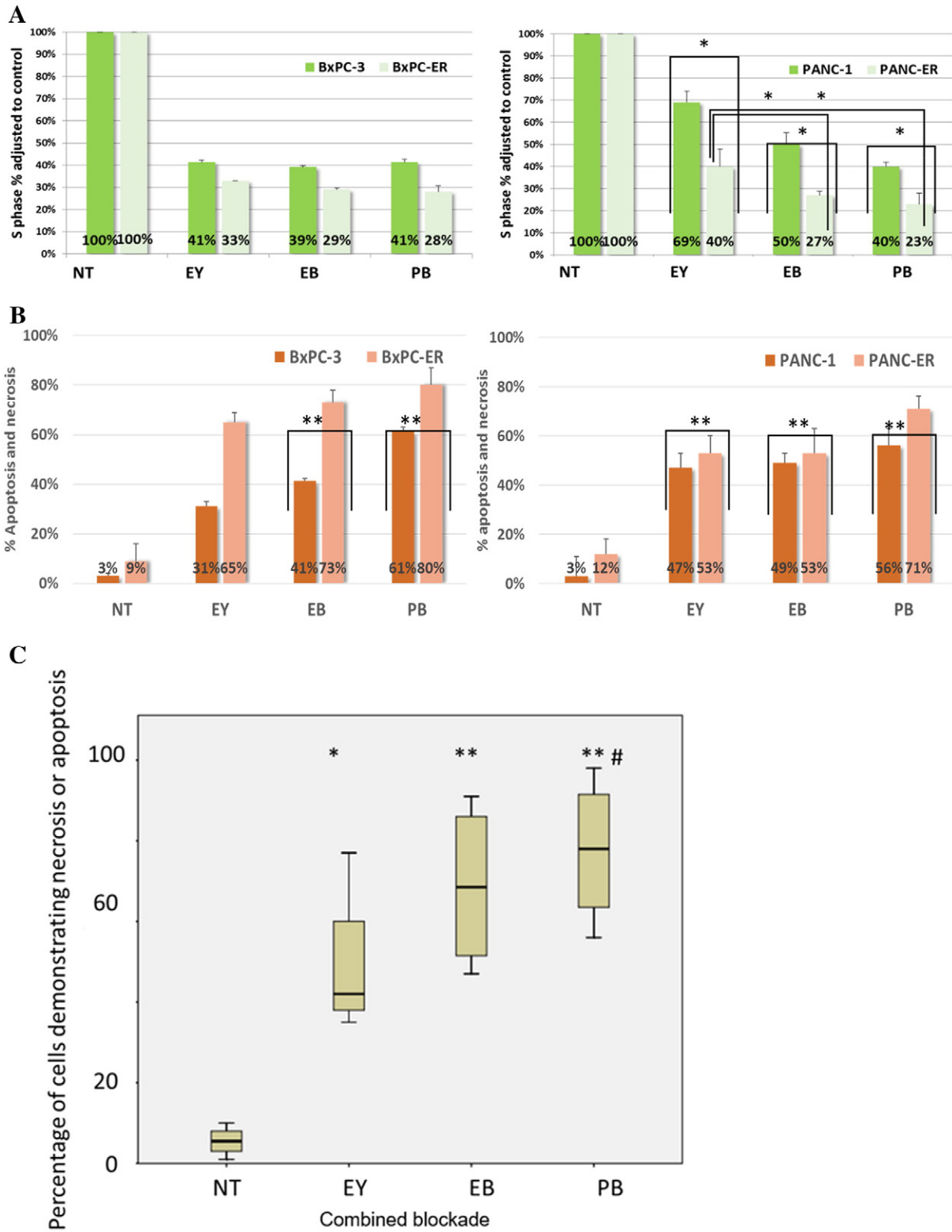
Figure 2. Effect of CB on cell cycle and apoptosis. (A) Effect of the CBs [EY, EB, and PD compared with no treatment (NT)] at low concentrations of ERL 5 μM, BYL719 2.5 μM, BEZ235 0.05 μM, and PD98059 5 μM on SPFs for ER cells and their parent cell lines. *$P < .05$.(B) Comparison of the effects of three CBs on the percentage of necrotic and apoptotic cells. EY denotes erlotinib plus BYL719, EB denotes erlotinib plus BEZ235, PB denotes PD98059 plus BEZ235. **$P < .01$.(C) Box-plot of the percentage of cells with necrosis or apoptosis and the effect of different treatments where NT is no treatment, and blockades of EGFR-PI3K as (EY), EGFR-PI3K/mTOR as (EB) and MEK-PI3K/mTOR as (PB). Differences between treatments and NT are indicated by * for $P < .01$ and ** for $P < .001$ and between EY and PB # = .05. *Post hoc* LSD significance analysis indicated all CBs to increase apoptosis and necrosis with a significantly greater effect of PB than EY ($P = .05$).
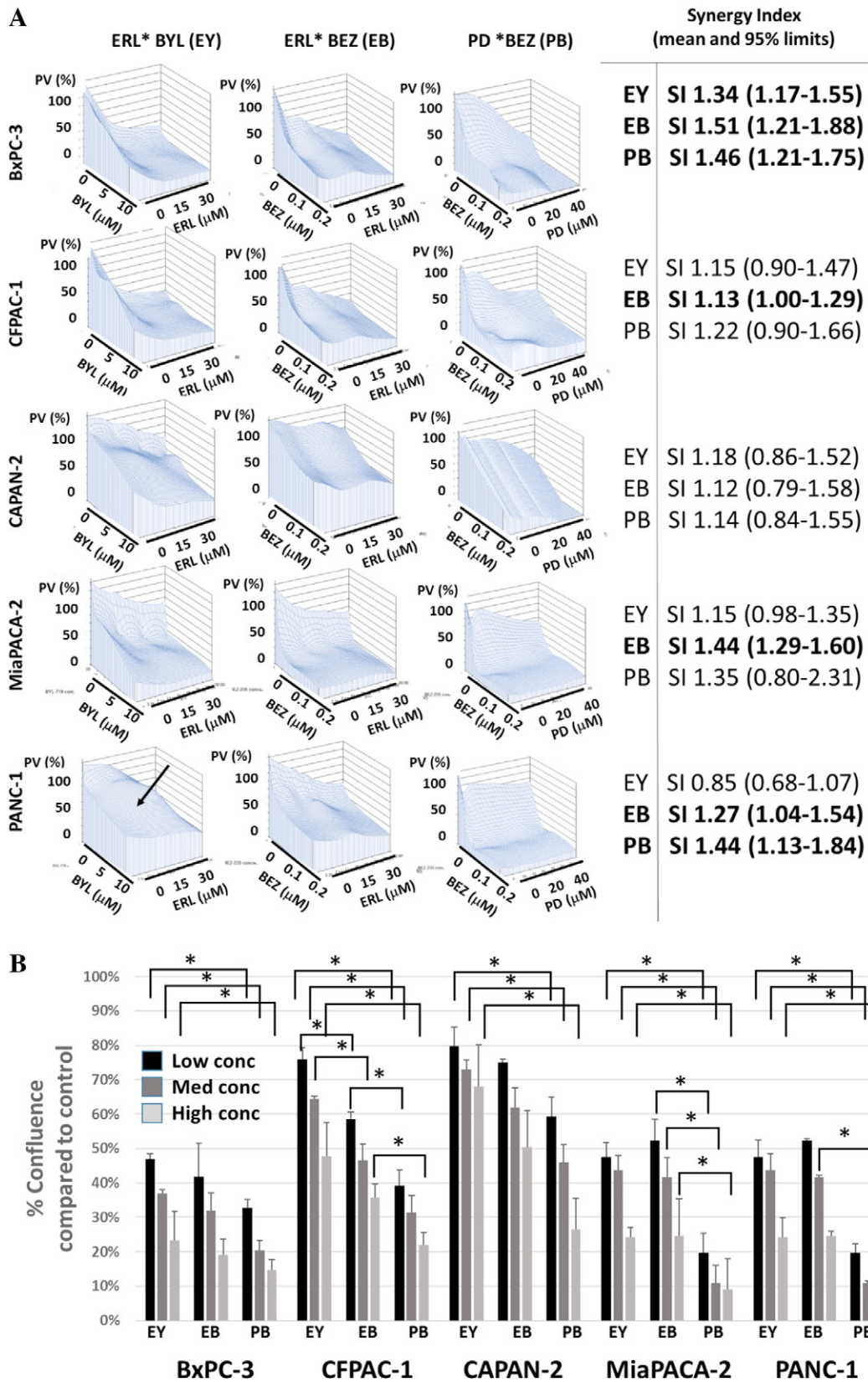
Figure 3. Synergistic effects of CB on cell proliferation. (A) Three-dimensional surface plots and respective SIs of three BCs on five PDAC cell lines. SI denotes synergy index, shown as mean values with 95% CI. PV denotes proportional viability. Arrow indicates convex contour on the three-dimensional surface plot suggesting antagonism. Values in bold indicate significant synergy ($P < .05$). (B) Percentage confluence under the influence of three CBs compared with control culture medium. Results of 3 doubling concentrations on 5 PDAC cell lines (ERL 5, 10, 20 μM; BYL 2.5, 5, 10 μM; BEZ 0.05, 0.1, 0.2 μM; PD 5, 10, 20 μM). Mean values $\pm$ SEM, *$P < .05$.

blockade. The three CBs were compared using low concentrations (ERL 5 µM/BYL 2.5 µM, ERL 5 µM/BEZ 0.05 µM, PD 5 µM/BEZ 0.05 µM) to demonstrate the differences in efficacy. All three CBs induced decreased SPF, probably reflecting G1-S cell cycle blockade, and there was a decrease in SPF following PB < EB < EY in three cell lines (BxPC-ER, PANC-1, PANC-ER), which was statistically significant in PANC-ER (EB < EY, *P* = .019; PB < EY, *P* = .027) (Figure 2*A*). A differential response was seen in each of the three CBs between PANC-ER and PANC-1 (EY, *P* = .022; EB, *P* = .035; PB, *P* = .050), in keeping with oncogenic dependence on PI3K/Akt in PANC-ER that was highly upregulated in this pathway.

With apoptosis assays, representative images showed a clear continuum from apoptosis (bottom left quadrant) to necrosis (bottom right quadrant) over a 72-hour treatment window

(Supplementary Figure 3). Although there was no clear pattern of increase in apoptosis or necrosis by the three CBs in these cell lines, taken together, there was an increasing trend toward increasing cell death by necrosis plus apoptosis caused by these CBs in all cell lines (PB > EB > EY). Pooled from quadruplicate experiments, the highest level of necrosis plus apoptosis was seen with the PB combination in all cell lines from 56% to 80%, followed by EB from 41% to 73% and lastly with EY from 31% to 65% (one-way analysis of variance, *P* = .03) (Figure 2*B*).When a two-way analysis of variance was undertaken, the influence of different CBs was highly significant (*P* = .002), but ER status was not (*P* = .3). *Post hoc* least significant difference analysis indicated that all CBs increase apoptosis and necrosis with a significantly greater effect of PB than EY (*P* = .05) (Figure 2*C*). Interestingly, ER status did not reduce the effect of CB
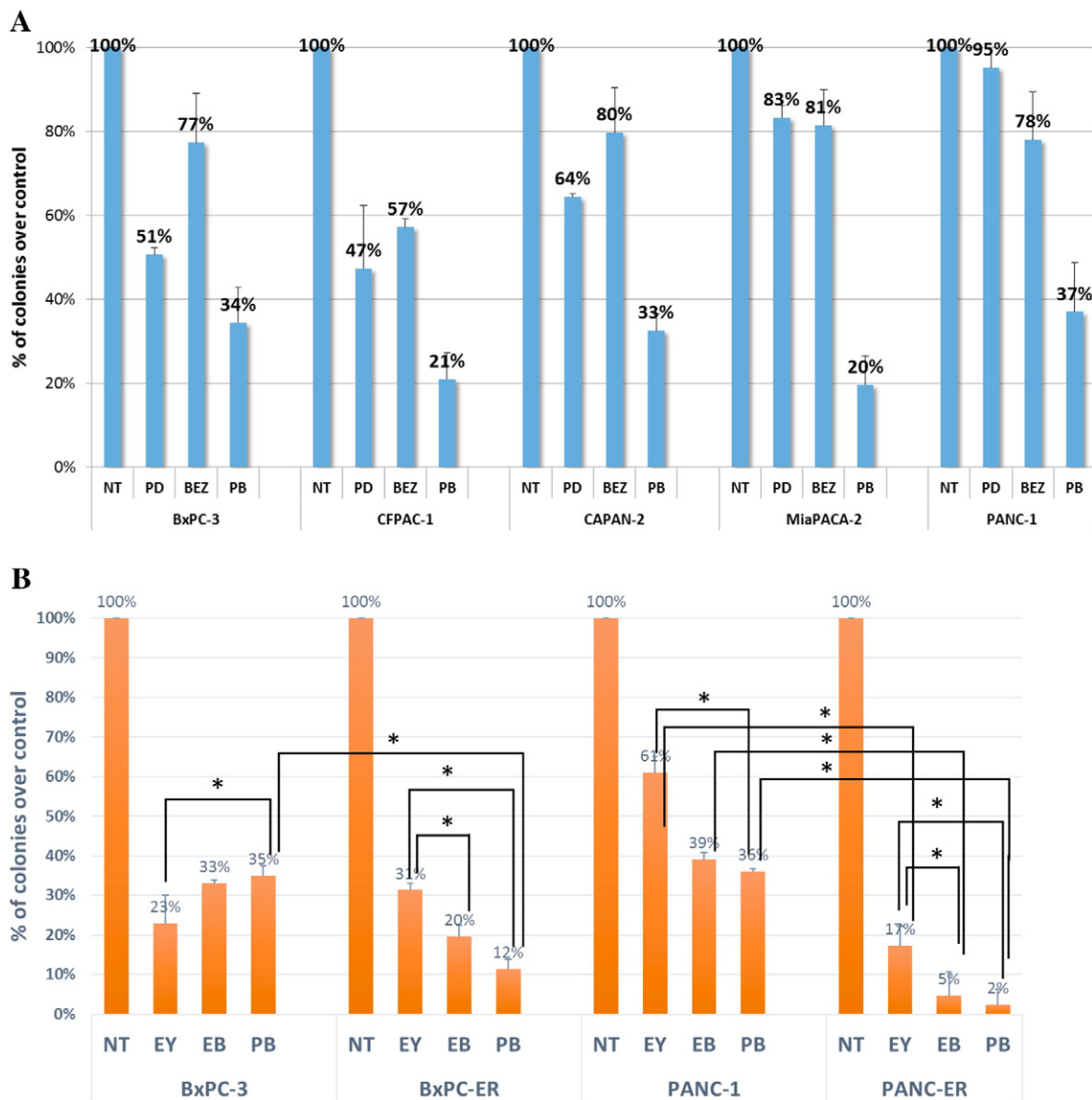

Figure 4. Effect of CB on clonogenic survival. (A) Mean and SEM of colony count as a percentage of untreated control for the effect of the PB combination on five PDAC cell lines. PD and BEZ were synergistic using the Bliss formula for all cell lines, *P < .05. (B) Comparison of three CBs on two pairs of parent and ER cell lines. Efficacy for PB was lower than that for EY in BxPC-3 cell line but higher in the other three cell lines (*P* < .05). In both ER cell lines, downstream CBs (EB and PB) suppressed colonies more effectively than in the respective parent cell lines (*P* < .05). Mean values ± SEM from four experiments.

on these measures, indicating that these CBs should remain effective despite prior erlotinib therapy.

Synergy and Efficacy Observed in Downstream CB

SIs were calculated and surface plots were created to test the additive effects of each drug on cell proliferation in the respective CB. This was tested across five primary PDAC cell lines and shown in Figure 3A. Significant synergy was found for all CBs in BxPC-3 likely because of the high sensitivity of this cell line to most drugs. Comparing the three CBs, significant synergy was found between ERL and BEZ in 4 out of 5 cell lines except for CAPAN-2, a cell line that was particularly slow in cell growth and cell death in 72-hour cell proliferation experiments. Although significant synergy was only demonstrated between PD and BEZ in two of five cell lines, the SIs closely approximated that between ERL and BEZ. EY in PANC-1 was the only combination with an SI <1, suggesting antagonism, which was characterized with a convex three-dimensional surface plot (straight arrow). However, in the pair of ER cell lines that became overactivated in PI3K/Akt, the EY combination trended toward greater synergy in the respective ER line, where mean SI and 95% CI changed from 0.85 (0.68-1.07) (PANC-1) to 1.44 (0.81-2.56) (PANC-ER) and from 1.34 (1.17-1.55) (BxPC-3) to 1.71 (1.00-2.89) (BxPC-ER), although these differences were not significant. Efficacy was studied by plotting the ratio of confluence of these cell lines treated with CBs compared with controls (Figure 3B). All cell lines demonstrated a decreasing trend of confluence or increasing efficacy in cell proliferation suppression in that PB > EB > EY. Significant differences were demonstrated between these CBs at most concentrations in CFPAC-1 and MiaPACA-2 in particular, and in all cell lines, PB significantly suppressed cell proliferation compared with EY in all concentrations (all Ps < .05).

Cell survival was studied using clonogenic assays. Given the slow-growing nature of CAPAN-2 and the lack of significant synergy found with the PB combination in cell proliferation experiments, particular focus was taken in testing this CB in clonogenic assays (Figure 4A). Single blockade by PD or BEZ was able to suppress colonies by 5% to 53% (average 32% for PD and 27% for BEZ), but the combination (PB) suppressed colonies by 63% to 80% (average 70%) The Bliss formula was used to assess for synergy. PD and BEZ were synergistic in all cell lines: BxPC-3 (expected 37% of colonies surviving, observed 34%), CFPAC-1 (expected 27%, observed 21%), CAPAN-2 (expected 51%, observed 33%), MiaPACA-2 (expected 67%, observed 20%), and PANC-1 (expected 74%, observed 37%). When the two ER cell lines were compared with their respective parent cell line, there appeared even fewer colonies formed in ER compared with parent cell lines (Supplementary Figure 4). Pooled from four experiments, there was significantly lower efficacy for PB compared with EY in the drug-sensitive BxPC-3 cell line only (Figure 4B). However, the three other cell lines showed significantly higher efficacy in PB compared with EY. In both ER cell lines, downstream CBs (EB and PB) suppressed colonies more than the respective parent cell lines, and significant differential responses were seen for all three CBs between PANC-1 and PANC-ER [P = .014 (EY), .004 (EB) and <.001 (PB)] as well as for PB between BxPC-3 and BxPC-ER (P = .001).

Finally, the effect of drug combinations on cell migration was tested because PI3K/Akt/mTOR has an important role in cancer cell migration [22,23]. Figure 5A shows an illustrative example of the effect of EY CB compared with ERL single blockade and control. Whereas cancer cells quickly apposed each other by 6 hours under control conditions, ERL delayed this process to 18 to 24 hours, whereas EY CB completely halted this process. When the three CBs were compared, they all significantly reduced migration to a similar extent particularly in BxPC-3 (50%-70%, all Ps < .01) and BxPC-ER (70%-90%, all Ps < .001) and less so in PANC-1 (20%-30%, all Ps < .05) and PANC-ER (20%-30%, all Ps < .05). PB performed slightly better than the other CBs, but this has not reached statistical significance (Figure 5B). Of note, in both BxPC-3 and BxPC-ER, the contour of the trend with all CBs was nearly completely flat beyond 20 hours compared with the near-exponential trend under control conditions. Although PB was slightly advantageous compared with EY and EB, it is clear that all CBs effectively suppressed migration of PDAC cells.

Discussion

The MAPK-PAM pathways are signaling cascades of kinases that play critical roles in cancer growth and proliferation [24]. The MAPK pathway is constitutively activated by mutated K-Ras through the intrinsic binding of GTPs in PDAC. K-Ras activates downstream signaling Raf (B-Raf, Raf-1, A-Raf), ERK, and MEK, which translocate into the cell nucleus, regulate transcription factors, and alter gene expression with the end result of promoting cell growth [24,25]. K-Ras mutation is present in increasing rates in advanced stages of pancreatic intraepithelial neoplasia (PanIN)—the precursor of PDAC—from 30% to 38% (PanIA), 31% to 44% (PanIB), and 73% (PanIN2) to 83% (PanIN3) and are prevalent in over 90% of PDAC [1]. The PAM pathway, on the other hand, is an integral pathway in cell growth and survival, responsible for important cellular functions such as protein synthesis, cell cycle progression, proliferation, and survival [26,27]. In PDAC, class I PI3-kinase is highly overexpressed in 70% of pancreatic ductal adenocarcinoma [28]. Akt, the direct downstream signal of the PI3K complex, is also consistently activated in over 40% of PDAC cell lines [29]. Once activated, Akt relieves the inhibition effect of TSC-1 and TSC-2 on the mTORC-1 and -2 complexes, leading to activation of direct downstream S6 and 4EBP-1, which are intricately involved in cell cycle and mRNA translation [30,31] (Supplementary Figure 1). Critical to the function of these two pathways is the myriad of upstream regulators including EGFR, IGF1R, and many others (e.g., MET or HGFR, HER2, VEGF-R, PDGF-R, Kit). Importantly, there is also significant interaction between the MAPK and PAM pathways at multiple levels, with interactions reported for K-Ras/GSK3β (a downstream effector of Akt), K-Ras/PTEN via TGF-β, and K-Ras/PI3K and PDK1 [32–35]. The multiple interactions and feedback loops certainly add a layer of complexity to the biology of these pathways and suggest that these signaling cascades should be viewed as a signaling network rather than a simple linear, unidirectional cascade [36]. Over the last decades, numerous novel inhibitors that inhibit the PAM pathways have now become available; many of these have entered into clinical studies, and a number of these have already been registered (Supplementary Figure 5). However, on their own, PAM pathway inhibitors have limited efficacy, and much effort is continuing to explore the best strategies to combine these agents [37]. Because a lot more is now understood about interactions between MAPK and PAM pathways, the current preclinical study was undertaken to explore upstream and downstream horizontal blockades in pancreatic cancer. The results of this study are summarized in Supplementary Table 2.
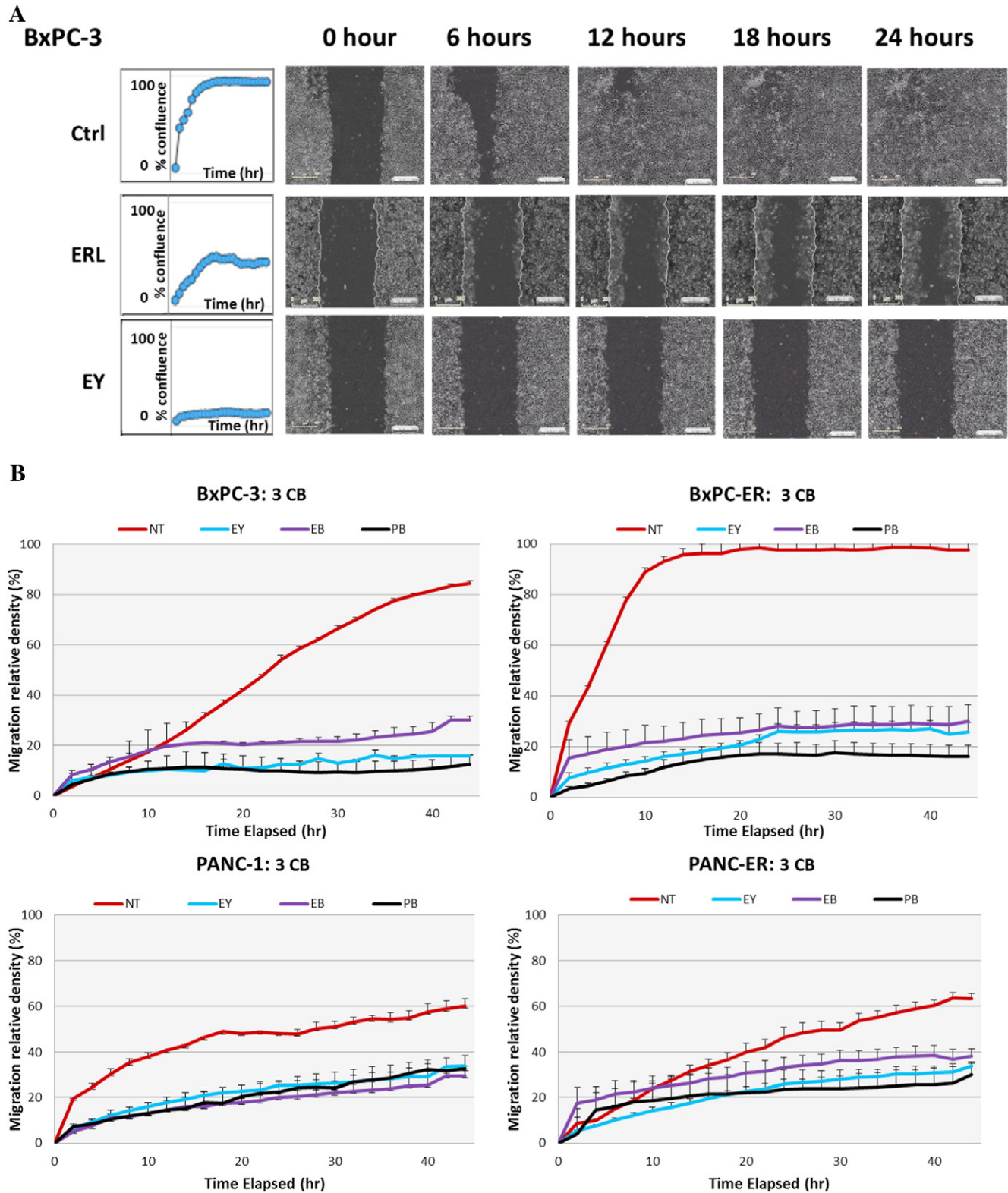
Figure 5. Migration assays: (A) Representative photographs of migration assays showing the effect of ERL 10 μM and the EY combination (10 μM/5 μM) on BxPC-3 cell line. The rate of migration was measured as the rates of increase in confluence after a uniform scratch was made by the 96-pin wound maker. (B) Effect of three drug combinations at medium concentrations (ERL 5 μM and BYL 5 μM, ERL 5 μM and BEZ 0.2 μM, PD 10 μM and BEZ 0.2 μM) on migration of the two pairs of parent and ER cell lines.

The first objective of the current study was to investigate the additional role of the downstream mediator mTOR in the cross-interaction between EGFR/MAPK and PAM pathways. For this reason, BEZ235—a dual PI3K/mTOR inhibitor—was chosen for *in vitro* experiments to directly compare with the PI3K inhibitor BYL719 in CB experiments. Western blotting experiments showed that BEZ-containing regimens (EB, PB) were more effective in attenuating pS6 than the BYL-containing regimen (EY), as expected

for a dual PI3K/mTOR inhibitor. In addition, in a representative example, these two CBs were also able to better suppress pERK and abrogate the pAkt signals in the two pairs of parent and ER cell lines, with statistically significant reduction shown in PANC-ER. This suggests that mTOR has a defined role in the interaction of MAPK-PAM pathways and that downstream CB is capable of switching off molecular signals of a cell line upregulated in PAM pathway. Further evidence for this came from cell proliferation and clonogenic survival experiments where significant synergy between ERL and BEZ was demonstrated in four out of five primary pancreatic cancer cell lines compared with only one out of five cell lines with significant synergy for the ERL-BYL combination and another cell line with possible antagonism. Although PD and BEZ were only significantly synergistic in two out of five cell lines, the SIs closely approximated those of ERL and BEZ. In the clonogenic assay experiments, all five PDAC cell lines showed significant synergy for this combination. Overall, these observations reinforced the close interaction between EGFR-downstream MAPK and PAM pathways via mTOR.

The second objective of the study was to further examine the mechanism of oncogenic dependence in PDAC cell lines. Previously, two primary cell lines that acquired resistance to EGFR (BxPC-ER and PANC-ER) had demonstrated upregulated *AKT2* and pAkt [16]. These in turn showed hypersensitivity when treated with EGFR and PI3K but not EGFR and IGF1R co-inhibition [16]. The current study sought to assess the differential effect of downstream MAPK/PAM pathway blockade on ER compared with parental cell lines. Significant differences were observed between ER and parent cell lines in cell cycle activity and clonogenic survival (PANC-1 and PANC-ER with all combinations) but not in migration assays. Cell survival and cell cycle are dominant functions of the PAM pathway via mTOR [20,21], so this may explain the significant differential response detected in these assays, pointing toward oncogenic dependence in these mechanisms. On the other hand, no differential patterns were shown in migration assay. Migration assay by its nature studied the immediate effect of treatment within the first 30 to 40 hours in contrast to cell proliferation and cell cycle assays (72 hours). As such, there may not be sufficient time for differential responses to be shown in the migration assay. In addition, migration is a highly complex cellular function that relies on numerous molecular mechanisms as well as cell-to-cell interaction rather than a sole molecular pathway [22,38,39]. In any case, these findings reinforce the notion that drug resistance can be overcome by co-targeting the original and the dominant onocogenic escape pathway, and may suggest a mechanism for achieving this through the abrogation of the molecular pathway (PAM pathway via mTOR) that the drug-resistant cell lines become addicted to.

Finally, this study sought to compare the efficacy between the three upstream and downstream MAPK-PAM CB regimens. In primary cell lines, cell proliferation assays showed increased drug efficacy in the order PB > EB > EY. Significant improvement in efficacy with PB compared with EY was demonstrated in all five PDAC cell lines. In the paired ER and parental cell line studies, there were also suggestive trends of increasing efficacy in cell cycle assays characterized by a decreasing trend in SPF (EY 33%-69%, EB 27%-50%, PB 23%-41%), in apoptosis assays characterized by increasing necrosis/apoptosis (EY 31%-65%, EB 41%-73%, PB 56%-80%), and in clonogenic assays with decreased colonies with the exception of BxPC-3 (EY 17%-61%, EB 5%-39%, PB 2%-36%). There was a significantly greater improvement with PB compared with EY shown on all four

parent:resistant cell line pairs in the clonogenic assay and in PANC-ER only in the cell cycle assay. Potential explanations of the efficacy of dual downstream blockade in PDAC include the facts that K-Ras mutation is present in 90% of PDAC [1] and that K-Ras activates the canonical MAPK pathway via Raf (B-Raf, Raf-1, A-Raf), ERK, and MEK [24] but also activates the PAM pathway directly via PI3K or indirectly through mediators such as GSK3β [32,35]. Although toxicity is clearly not able to be adequately explored in preclinical studies, these findings support clinical development of dual inhibitors with downstream blockade of MAPK and PAM in PDAC, which reinforces existing evidence in this field [40–42].

In summary, this study finds close interaction between MAPK and PAM pathways via mTOR in pancreatic cancer, reinforcing that drug resistance may be overcome by inhibition of oncogenic-dependent pathways, and suggests dual MEK and PI3K/mTOR blockade as an attractive therapeutic target in pancreatic cancer.

Funding

Appendix A. Supplementary data

Supplementary data to this article can be found online at http://dx.doi.org/10.1016/j.neo.2016.06.001.

References

[1] Schneider G and Schmid RM (2003). Genetic Alterations in Pancreatic Carcinoma. *Mol Cancer* **2**, 15.

[2] Li J (2013). Genetic Epidemiology and Pancreatic Cancer. In: Simone D, Maitra A, editors. Molecular Genetics of Pancreatic Cancer. New York: Springer; 2013 [Chapter 3].

[3] Bardeesy N and Depinho RA (2002). Pancreatic Cancer Biology and Genetics. *Nat Rev Cancer* **2**, 897–909.

[4] Moore MJ, Goldstein D, Hamm J, Figer A, Hecht JR, Gallinger S, Au HJ, Murawa P, Walde D, and Wolff RA, et al (2007). Erlotinib Plus Gemcitabine Compared With Gemcitabine Alone in Patients With Advanced Pancreatic Cancer: a Phase III Trial of the National Cancer Institute of Canada Clinical Trials Group. *J Clin Oncol* **25**, 1960–1966.

[5] Burrell RA, McGranahan N, Bartek J, and Swanton C (2013). The Causes and Consequences of Genetic Heterogeneity in Cancer Evolution. *Nature* **501**, 338–345.

[6] Biankin AV, Waddell N, Kassahn KS, Gingras MC, Muthuswamy LB, Johns AL, Miller DK, Wilson PJ, Patch AM, and Wu J, et al (2012). Pancreatic Cancer Genomes Reveal Aberrations in Axon Guidance Pathway Genes. *Nature* **491**, 399–405.

[7] Yachida S, Jones S, Bozic I, Antal T, Leary R, Fu B, Kamiyama M, Hruban RH, Eshleman JR, and Nowak MA, et al (2010). Distant Metastasis Occurs Late During the Genetic Evolution of Pancreatic Cancer. *Nature* **467**, 1114–1117.

[8] da Cunha SG, Dhani N, Tu D, Chin K, Ludkovski O, Kamel-Reid S, Squire J, Parulekar W, Moore MJ, and Tsao MS (2010). Molecular Predictors of Outcome in a Phase 3 Study of Gemcitabine and Erlotinib Therapy in Patients With Advanced Pancreatic Cancer: National Cancer Institute of Canada Clinical Trials Group Study PA.3. *Cancer* **116**, 5599–5607.

[9] Greenhalf W, Ghaneh P, Neoptolemos JP, Palmer DH, Cox TF, Lamb RF, Garner E, Campbell F, Mackey JR, and Costello E, et al (2014). Pancreatic Cancer HENT1 Expression and Survival From Gemcitabine in Patients From the ESPAC-3 Trial. *J Natl Cancer Inst* **106**, djt347.

[10] Sinn M, Riess H, Sinn BV, Stieler JM, Pelzer U, Striefler JK, Oettle H, Bahra M, Denkert C, and Blaker H, et al (2015). Human Equilibrative Nucleoside Transporter 1 Expression Analysed by the Clone SP 120 Rabbit Antibody Is Not Predictive in Patients With Pancreatic Cancer Treated With Adjuvant Gemcitabine - Results From the CONKO-001 Trial. *Eur J Cancer* **51**, 1546–1554.

[11] Hidalgo M, Plaza C, Musteanu M, Illei P, Brachmann CB, Heise C, Pierce D, Lopez-Casas PP, Menendez C, and Tabernero J, et al (2015). SPARC Expression Did Not Predict Efficacy of Nab-Paclitaxel Plus Gemcitabine or Gemcitabine Alone for Metastatic Pancreatic Cancer in an Exploratory Analysis of the Phase III MPACT Trial. *Clin Cancer Res* **21**, 4811–4818.

[12] Huang ZQ, Saluja AK, Dudeja V, Vickers SM, and Buchsbaum DJ (2011). Molecular Targeted Approaches for Treatment of Pancreatic Cancer. *Curr Pharm Des* **17**, 2221–2238.

[13] Britten CD (2013). PI3K and MEK Inhibitor Combinations: Examining the Evidence in Selected Tumor Types. *Cancer Chemother Pharmacol* **71**, 1395–1409.

[14] Chappell WH, Steelman LS, Long JM, Kempf RC, Abrams SL, Franklin RA, Basecke J, Stivala F, Donia M, and Fagone P, et al (2011). Ras/Raf/MEK/ERK and PI3K/PTEN/Akt/MTOR Inhibitors: Rationale and Importance to Inhibiting These Pathways in Human Health. *Oncotarget* **2**, 135–164.

[15] Sos ML, Fischer S, Ullrich R, Peifer M, Heuckmann JM, Koker M, Heynck S, Stuckrath I, Weiss J, and Fischer F, et al (2009). Identifying Genotype-Dependent Efficacy of Single and Combined. *Proc Natl Acad Sci U S A* **106**, 18351–18356.

[16] Wong MH, Xue A, Julovi SM, Pavlakis N, Samra JS, Hugh TJ, Gill AJ, Peters L, Baxter RC, and Smith RC (2014). Cotargeting of Epidermal Growth Factor Receptor and PI3K Overcomes PI3K-Akt Oncogenic Dependence in Pancreatic Ductal Adenocarcinoma. *Clin Cancer Res* **20**, 4047–4058.

[17] Sylvester PW (2011). Optimization of the Tetrazolium Dye (MTT) Colorimetric Assay for Cellular Growth and Viability. *Methods Mol Biol* **716**, 157–168.

[18] Whitehead A, Whitehead J, Todd S, Zhou Y, and Smith MK (2008). Fitting Models for the Joint Action of Two Drugs Using SAS. *Pharm Stat* **7**, 272–284.

[19] Yao E, Zhou W, Lee-Hoeflich ST, Truong T, Haverty PM, Eastham-Anderson J, Lewin-Koh N, Gunter B, Belvin M, and Murray LJ, et al (2009). Suppression of HER2/HER3-Mediated Growth of Breast Cancer Cells With Combinations of GDC-0941 PI3K Inhibitor, Trastuzumab, and Pertuzumab. *Clin Cancer Res* **15**, 4147–4156.

[20] Fingar DC, Richardson CJ, Tee AR, Cheatham L, Tsou C, and Blenis J (2004). MTOR Controls Cell Cycle Progression Through Its Cell Growth Effectors S6K1 and 4E-BP1/Eukaryotic Translation Initiation Factor 4E. *Mol Cell Biol* **24**, 200–216.

[21] Castedo M, Ferri KF, and Kroemer G (2002). Mammalian Target of Rapamycin (MTOR): Pro- and Anti-Apoptotic. *Cell Death Differ* **9**, 99–100.

[22] Zhang X, Shi H, Tang H, Fang Z, Wang J, and Cui S (2015). MiR-218 Inhibits the Invasion and Migration of Colon Cancer Cells by Targeting the PI3K/Akt/MTOR Signaling Pathway. *Int J Mol Med* **35**, 1301–1308.

[23] Huang CY, Fong YC, Lee CY, Chen MY, Tsai HC, Hsu HC, and Tang CH (2009). CCL5 Increases Lung Cancer Migration Via PI3K, Akt and NF-KappaB Pathways. *Biochem Pharmacol* **77**, 794–803.

[24] Steelman LS, Franklin RA, Abrams SL, Chappell W, Kempf CR, Basecke J, Stivala F, Donia M, Fagone P, and Nicoletti F, et al (2011). Roles of the Ras/Raf/MEK/ERK Pathway in Leukemia Therapy. *Leukemia* **25**, 1080–1094.

[25] Furukawa T, Sunamura M, and Horii A (2006). Molecular Mechanisms of Pancreatic Carcinogenesis. *Cancer Sci* **97**, 1–7.

[26] Fresno Vara JA, Casado E, de CJ, Cejas P, Belda-Iniesta C, and Gonzalez-Baron M (2004). PI3K/Akt Signalling Pathway and Cancer. *Cancer Treat Rev* **30**, 193–204.

[27] Paez J and Sellers W (2003). R. PI3K/PTEN/AKT Pathway. A Critical Mediator of Oncogenic Signaling. *Cancer Treat Res* **115**, 145–167.

[28] Edling CE, Selvaggi F, Buus R, Maffucci T, Di SP, Friess H, Innocenti P, Kocher HM, and Falasca M (2010). Key Role of Phosphoinositide 3-Kinase Class IB in Pancreatic Cancer. *Clin Cancer Res* **16**, 4928–4937.

[29] Bondar VM, Sweeney-Gotsch B, Andreeff M, Mills GB, and McConkey DJ (2002). Inhibition of the Phosphatidylinositol 3'-Kinase-AKT Pathway Induces Apoptosis in Pancreatic Carcinoma Cells in Vitro and in Vivo. *Mol Cancer Ther* **1**, 989–997.

[30] Hay N and Sonenberg N (2004). Upstream and Downstream of MTOR. *Genes Dev* **18**, 1926–1945.

[31] Huang J and Manning BD (2009). A Complex Interplay Between Akt, TSC2 and the Two MTOR Complexes. *Biochem Soc Trans* **37**, 217–222.

[32] Zhang JS, Koenig A, Harrison A, Ugolkov AV, Fernandez-Zapico ME, Couch FJ, and Billadeau DD (2011). Mutant K-Ras Increases GSK-3beta Gene Expression Via an ETS-P300 Transcriptional Complex in Pancreatic Cancer. *Oncogene* **30**, 3705–3715.

[33] Chow JY, Quach KT, Cabrera BL, Cabral JA, Beck SE, and Carethers JM (2007). RAS/ERK Modulates TGFbeta-Regulated PTEN Expression in Human Pancreatic Adenocarcinoma Cells. *Carcinogenesis* **28**, 2321–2327.

[34] Eser S, Reiff N, Messer M, Seidler B, Gottschalk K, Dobler M, Hieber M, Arbeiter A, Klein S, and Kong B, et al (2013). Selective Requirement of PI3K/PDK1 Signaling for Kras Oncogene-Driven Pancreatic Cell Plasticity and Cancer. *Cancer Cell* **23**, 406–420.

[35] Yang HW, Shin MG, Lee S, Kim JR, Park WS, Cho KH, Meyer T, and Heo WD (2012). Cooperative Activation of PI3K by Ras and Rho Family Small GTPases. *Mol Cell* **47**, 281–290.

[36] Roberts PJ and Der CJ (2007). Targeting the Raf-MEK-ERK Mitogen-Activated Protein Kinase Cascade for the Treatment of Cancer. *Oncogene* **26**, 3291–3310.

[37] Cho DC (2014). Targeting the PI3K/Akt/MTOR Pathway in Malignancy: Rationale and Clinical Outlook. *BioDrugs* **28**, 373–381.

[38] Giehl K, Imamichi Y, and Menke A (2007). Smad4-Independent TGF-Beta Signaling in Tumor Cell Migration. *Cells Tissues Organs* **185**, 123–130.

[39] Haque I, Mehta S, Majumder M, Dhar K, De A, McGregor D, Van Veldhuizen PJ, Banerjee SK, and Banerjee S (2011). Cyr61/CCN1 Signaling Is Critical for Epithelial-Mesenchymal Transition and Stemness and Promotes Pancreatic Carcinogenesis. *Mol Cancer* **10**, 8.

[40] Williams TM, Flecha AR, Keller P, Ram A, Karnak D, Galban S, Galban CJ, Ross BD, Lawrence TS, and Rehemtulla A, et al (2012). Cotargeting MAPK and PI3K Signaling With Concurrent Radiotherapy As a Strategy for the Treatment of Pancreatic Cancer. *Mol Cancer Ther* **11**, 1193–1202.

[41] Roy SK, Srivastava RK, and Shankar S (2010). Inhibition of PI3K/AKT and MAPK/ERK Pathways Causes Activation of FOXO Transcription Factor, Leading to Cell Cycle Arrest and Apoptosis in Pancreatic Cancer. *J Mol Signal* **5**, 10.

[42] Eser S, Schnieke A, Schneider G, and Saur D (2014). Oncogenic KRAS Signalling in Pancreatic Cancer. *Br J Cancer* **111**, 817–822.